



IUTAM Symposium on Multiphase flows with phase change: challenges and opportunities,
Hyderabad, India (December 08 – December 11, 2014)

Numerical modelling of melt behaviour in the lower vessel head of a nuclear reactor

D. Pavlidis^{a,*}, J. L. M. A. Gomes^b, Z. Xie^c, C. C. Pain^a, A. A. K. Tehrani^d,
M. Moatamedi^e, P. N. Smith^a, A. V. Jones^a, O. K. Matar^c

^aDept. Earth Science & Engineering, Imperial College London, London SW7 2AZ, UK

^bSchool of Engineering, University of Aberdeen, Aberdeen AB24 3UE, UK

^cDept. Chemical Engineering, Imperial College London, London SW7 2AZ, UK

^dOffice for Nuclear Regulation, Bootle L20 7HS, UK

^eCentre for Nuclear Engineering, Imperial College London, London SW7 2AZ, UK

Abstract

This paper describes progress on a consistent approach for multi-phase flow modelling with phase-change. Although, the developed methods are general purpose the applications presented here cover the LIVE experiments involving core melt phenomena at the lower vessel head of a nuclear reactor. These include corium pool formation, coolability and solidification. A new method for solving the compositional multi-phase flow equations to calculate material indicator fields is adopted. An interface-capturing scheme based on high-order accurate compressive advection methods including a Petrov-Galerkin approach is employed to maintain sharpness of the interfaces between materials. A novel control volume-finite element mixed formulation based on the P_1 DG- P_2 (linear discontinuous in velocity and quadratic continuous in pressure) element pair which can uniquely ensure that key balances are maintained in the equations is developed to discretise the governing equations in space. Anisotropic mesh adaptivity is used to focus the numerical resolution around the interfaces and other areas of important dynamics.

© 2015 The Authors. Published by Elsevier B.V. This is an open access article under the CC BY-NC-ND license (<http://creativecommons.org/licenses/by-nc-nd/4.0/>).

Peer-review under responsibility of Indian Institute of Technology, Hyderabad.

Keywords:

Heat transfer; melt pool; phase-change; solidification.

1. Introduction

Understanding the thermal-hydraulic behaviour of corium pool in the reactor pressure vessel (RPV) lower head of pressurised water reactors during core melt accidents is of significance in reactor safety. The LIVE experiments¹ are being undertaken at Karlsruhe Institute of Technology, Germany for this reason.

Numerically reproducing the aforementioned experiments requires advanced thermal-hydraulics models that support multi-material modelling (interface tracking or capturing), allow for different equations of state (compressible

* Corresponding author. Tel.: +44-020-7594-9986.

E-mail address: dimitrios.pavlidis@imperial.ac.uk

fluids/expanding solids) to be assigned to each material, include complex rheologies and account for chemical processes in the system. In this study, developments towards numerically modelling these experiments are presented. Emphasis is given on interface capturing for arbitrary number of materials with different equations of state and phase-change.

The motivation for this work is to exploit state-of-the-art methods for multi-fluids modelling with interface-capturing numerical schemes. These include:

- (a) Multi-component modelling that embeds information on interfaces into the continuity equations. Advantages of this approach are:
 - (i) The model is designed for compressible multi-fluid flows with arbitrary number of fluids/materials, and does not rely on priority list of materials (common for traditional multi-material models), which often produces spurious solutions² and;
 - (ii) The component advection equations are embedded into both pressure and continuity equations resulting in local mass balance (within each control volume).
- (b) Use of new type of triangle/tetrahedron finite elements^{3,4}, in particular the P₁DG-P₂ (element-wise linear velocity, discontinuous across element interfaces and element-wise quadratic pressure). This family of elements has velocity mass matrices local to each element which enables them to be inverted easily and the results are embedded into the pressure matrix equation which is formed by a projection method. In addition, key balances, such as the vertical pressure gradient and buoyancy force balance, are enforced exactly.
- (c) Novel interface-capturing scheme based on high-order accurate compressive advection methods. A down-winding scheme is formulated using a high-order finite element method to obtain fluxes on the control volume boundaries which are subject to flux-limiting using a normalised variable diagram approach^{5,6,7} to obtain bounded and compressive (capturing the interfaces) solutions. The approach uses a novel two-level time stepping method which allows large time steps to be used while maintaining stability and boundedness.
- (d) A non-linear Petrov-Galerkin method is used as an implicit large-eddy simulation that resolves as much of the structure in the flow as possible, and controls numerical oscillations.
- (e) The method is coupled to an anisotropic mesh adaptivity algorithm⁸, which maximises computational efficiency by dynamically refining or coarsening the computational mesh to minimise predicted interpolation error as the simulation progresses. Unlike adaptive mesh refinement methods based on Cartesian grid bisection, as previously applied to multi-phase simulation⁹, the algorithm produces smoothly gradated meshes which naturally align with flow structures.

The remainder of this paper is organised as follows. A brief description of the model is given in section 2 and preliminary results are presented in section 3. Finally, some concluding remarks are given in section 4.

2. Governing equations

In multi-component flows, a number of components exist in one or more phases (one phase is assumed here but is easily generalised to an arbitrary number of phases). Let α_i be the volume fraction of component i , where $i = 1, 2, \dots, N_c$. N_c denotes the number of components. The density of component i is ρ_i . A constraint on the system is:

$$\sum_{i=1}^{N_c} \alpha_i = 1. \quad (1)$$

For each fluid component i the conservation of mass may be defined as:

$$\frac{\partial}{\partial t}(\alpha_i \rho_i) + \nabla \cdot (\alpha_i \rho_i \mathbf{u}) = Q_i, \quad i = 1, 2, \dots, N_c, \quad (2)$$

where t , \mathbf{u} and Q_i are the time, velocity vector field and mass source term, respectively. The equations of motion of a compressible viscous fluid may be written as:

$$\frac{\partial}{\partial t}(\rho \mathbf{u}) + \nabla \cdot (\rho \mathbf{u} \mathbf{u}) = -\nabla p + \nabla \cdot \mu (\nabla \mathbf{u} + \nabla^T \mathbf{u}) - \nabla \frac{2}{3} \mu \nabla \cdot \mathbf{u} + \rho g \mathbf{k}, \quad (3)$$

where p is the pressure, the bulk density is $\rho = \sum_{i=1}^{N_c} \alpha_i \rho_i$, the bulk viscosity is $\mu = \sum_{i=1}^{N_c} \alpha_i \mu_i$, g is the gravitational acceleration and \mathbf{k} is a unit vector pointing in the direction of gravity.

The temperature equation is:

$$\rho C_p \frac{\partial}{\partial t} T + \rho C_p \nabla \cdot (\mathbf{u} T) = +\nabla \cdot \kappa \nabla T + Q^T, \quad (4)$$

where the bulk heat capacity is $C_p = \sum_{i=1}^{N_c} \alpha_i C_{p_i}$, the bulk thermal conductivity is $\kappa = \sum_{i=1}^{N_c} \alpha_i \kappa_i$ and Q^T is a heat source term.

The spatial discretisation of the momentum equation is described in detail in⁴. Details on the compositional modelling approach, the derivation of the global continuity equation and the overall solution method can be found in¹⁰.

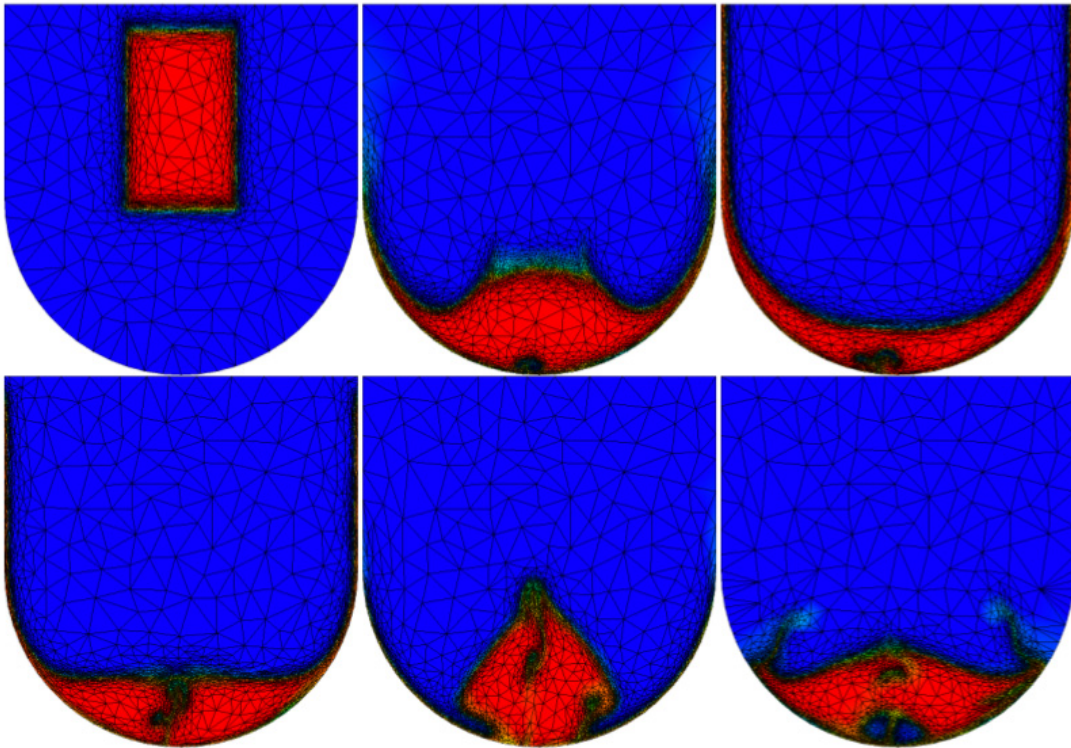


Fig. 1. Instantaneous maps of the corium simulant field along with the mesh at six time levels for the first stage (molten material collapse under gravity) of the 2D LIVE experiment. The molten material is represented by red and air is represented by blue. Time levels t from top left to bottom right: 0.074, 0.392, 0.692, 0.981, 1.23 and 1.45s.

3. Results

The model is applied to parts of the LIVE-L1 experiment¹. LIVE-L1 is aimed at investigating the melt pool and crust behaviour during the stages of air circulation at the outer RPV surface with subsequent flooding of the lower

head. The simulation is divided into two parts. The first part simulates the collapsing, sloshing and settling of the molten material onto the lower vessel head. The second part simulates the cooling and solidification of the molten salt and is dominated by convection. The first part is simulated in two dimensions and the second part is simulated in three dimensions.

3.1. First part

For the first simulation; the computational domain consists of a semicircle of radius 0.5m, which represents the lower vessel head, below a rectangle of dimensions 1m×0.55m. The molten material initial dimensions are 0.3m×0.5m which is placed at the geometry centreline, 0.05m under the domain top boundary (see Fig. 1, top left). This column collapses under gravity freely to the lower head at the beginning of the transient. It is however noted that in the LIVE test facility the corium simulant is injected at a specified flow rate which is not included in this study.

The air density is set to $\approx 0.56\text{kg/m}^3$ (assumed incompressible perfect gas at 350°C) and the air viscosity is set to 10^{-3}kg/(ms) . The molten material density is set to 1868kg/m^3 and the molten material viscosity is set to 10^{-3}kg/(ms) .

Instantaneous maps of the corium simulant along with the mesh at six time levels ($t = 0.074, 0.392, 0.692, 0.981, 1.23$ and 1.45s) for the first stage (molten material collapse under gravity) of the LIVE experiment are shown in Fig. 1. The molten material is represented by red and air is represented by blue. The adaptive mesh simulation is able to efficiently resolve the air-corium simulant interface while drastically reducing the computational cost.

3.2. Second part

For the second simulation the computational domain consists of the lower part of a semi-sphere of radius 0.5m with height 0.31m (same melt height as in the LIVE-L1 experiment). The domain is fully saturated with molten material.

A free-slip boundary condition is weakly enforced on the bottom boundary, while absorption equal to $\rho/\Delta t$ on the vertical component of velocity acts as a free surface. The pressure level at the top boundary is set to atmospheric pressure. The temperature field is initialised to 350C. A 10KW volumetric heat source is also applied uniformly, throughout the domain. Heat is removed from the bottom boundary through a Robin boundary condition of the form: $\mathbf{n} \cdot (\kappa \nabla T) = h(T_{\text{ref}} - T)$, where \mathbf{n} is the outward-pointing unit vector from the domain boundary, h is the interfacial heat transfer coefficient and $T_{\text{ref}} = 150^\circ\text{C}$ is a reference wall temperature.

The coefficient h is calculated through $h = \kappa Nu/d$, where the length scale d is 1m, the thermal conductivity κ is set to 0.5W/(mK) and:

$$Nu = 0.68 + \frac{0.67Ra^{0.25}}{\left(1 + (0.492/Pr)^{0.5625}\right)^{0.444}}, \quad (5)$$

where Ra is the Rayleigh number and Pr is the Prandtl number. The Ra number is a function of the angle between domain boundary outward-pointing vector and the horizontal.

The molten material density is calculated through: $\rho = \rho_o \left(1 - 2 \times 10^{-4} (T - T_o)\right) \text{kg/m}^3$, where $\rho_o = 1868\text{kg/m}^3$ and $T_o = 350^\circ\text{C}$. The thermal expansion coefficient 2×10^{-4} assumes a 2% change in volume every 100°C . The molten material viscosity is set to 10^{-3}kg/(ms) if $T > 280^\circ\text{C}$ and 10^6kg/(ms) if $T < 220^\circ\text{C}$. Linear interpolation is used to determine the viscosity if the temperature is between 220 and 280°C . Latent heat is introduced through temperature-dependant heat capacity and heat capacities are adopted from¹¹.

A 5×10^4 -element, unstructured, fixed mesh of approximately equally sized elements is used for this simulation.

Instantaneous maps of the temperature and velocity fields at four time levels for the second stage (molten material cooling/solidification) of the LIVE experiment are shown in Fig. 2. Effects of buoyancy are evident on the velocity field (recirculation). The lowest wall temperatures are found near the centreline which is where the crust is thickest (zero velocity areas in Figure 4, right). This is consistent with the experimental results, see¹. The growth of the crust thickness in time is evident.

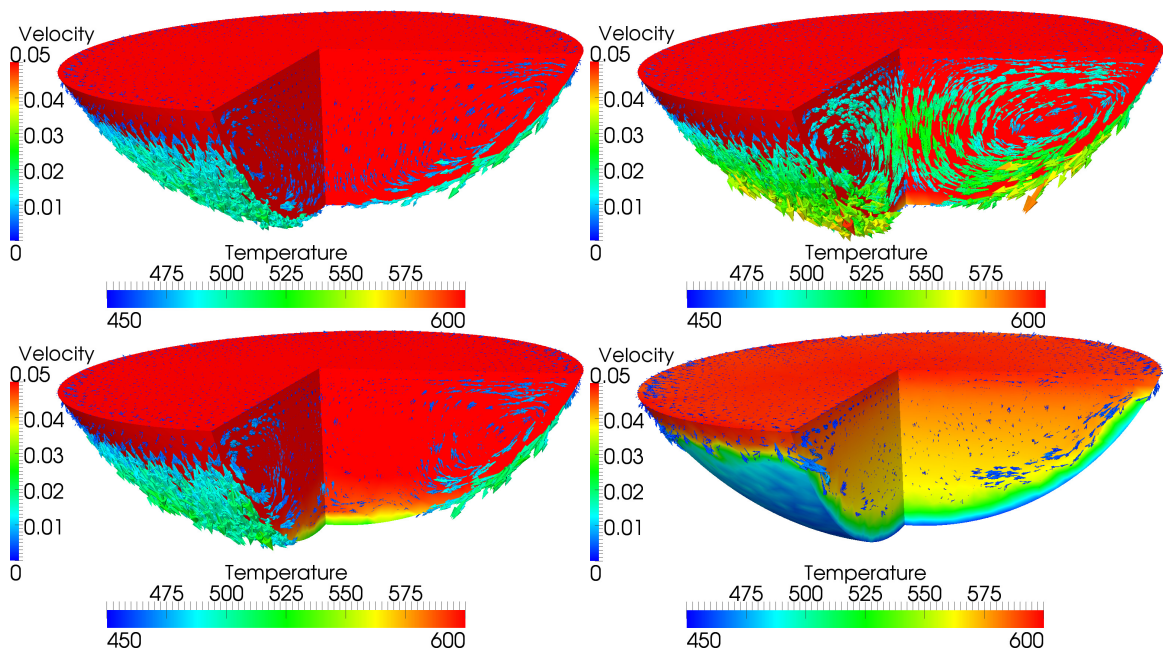


Fig. 2. Instantaneous maps of the temperature and velocity fields at four time levels for the second stage (molten material cooling/solidification) of the LIVE experiment. The units of temperature and velocity are K and in m/s, respectively. Time levels t from top left to bottom right: 3, 10, 35 and 650s.

4. Conclusions

A method for numerically simulating multi-phase flows of arbitrary numbers of phases including arbitrary equations of state assigned to each phase and phase-change has been briefly outlined here. Some features have been demonstrated through the LIVE experiment simulations.

Acknowledgements

The authors would like to thank the EPSRC MEMPHIS multi-phase programme grant, the EPSRC Computational modelling for advanced nuclear power plants project and the EU FP7 projects THINS and GoFastR for helping to fund this work.

References

1. Fluhner, B., Miassoedov, A., Cron, T., Foit, J., Gaus-Liu, X., Schmidt-Stiefel, S., et al. The LIVE-L1 and LIVE-L3 experiments on melt behaviour in RPV lower head. Tech. Rep.; Forschungszentrum Karlsruhe GmbH; Karlsruhe, Germany; 2009.
2. Wilson, C.. *Modelling multiple-material flows on adaptive unstructured meshes*. Ph.D. thesis; Department of Earth Science and Engineering, Imperial College London; 2009.
3. Cotter, C.J., Ham, D.A., Pain, C.C., Reich, S.. LBB stability of a mixed Galerkin finite element pair for fluid flow simulations. *Journal of Computational Physics* 2009;**228**:336–348.
4. Cotter, C.J., Ham, D.A., Pain, C.C.. A mixed discontinuous/continuous finite element pair for shallow-water ocean modelling. *Ocean Modelling* 2009;**26**:86–90.
5. Leonard, B.P.. The ULTIMATE conservative difference scheme applied to unsteady one-dimensional advection. *Computer Methods in Applied Mechanics and Engineering* 1991;**88**:17–74.
6. Darwish, M.S.. A new high-resolution scheme based on the normalized variable formulation. *Numerical Heat Transfer - Part B* 1993; **24**:353–371.
7. Darwish, M., Moukalled, F.. The χ -schemes: a new consistent high-resolution based on the normalised variable methodology. *Computer Methods in Applied Mechanics and Engineering* 2003;**192**:1711–1730.

8. Pain, C.C., Umpleby, A.P., de Oliveira, C.R.E., Goddard, A.J.H.. Tetrahedral mesh optimisation and adaptivity for steady-state and transient finite element calculations. *Computer Methods in Applied Mechanics and Engineering* 2001;**190**:3771–3796.
9. Chen, X., Yang, V.. Thickness-based adaptive mesh refinement methods for multi-phase flow simulations with thin regions. *Journal of Computational Physics* 2014;**269**(0):22 – 39.
10. Pavlidis, D., Xie, Z., Percival, J.R., Gomes, J.L.M.A., Pain, C.C., Matar, O.K.. Two- and three-phase horizontal slug flow simulations using an interface-capturing compositional approach. *International Journal of Multiphase Flow* 2014;In press.
11. Carling, R.W.. Heat capacities of NaNO_3 and KNO_3 from 350 to 800K. *Thermochimica Acta* 1983;**60**:265–275.